

# The role of MHD in the sustainment of electron internal transport barriers and H-mode in TCV

G. Turri , O. Sauter, S. Alberti, E. Asp, T.P. Goodman, L. Porte, V.S. Udintsev, C. Zucca

Ecole Polytechnique Fédérale de Lausanne (EPFL) Centre de Recherches en Physique des Plasmas, Association Euratom-Confederation Suisse CH-1015 Lausanne, Switzerland.

E-mail: Gianpaolo.Turri@epfl.ch, Olivier.Sauter@epfl.ch

**Abstract.** Advanced scenarios exhibit improved confinement properties, which make them attractive candidate for ITER. For these to be achieved, the sustainment of transport barriers and therefore high pressure gradients is inherent. Their stability properties both in the transient and steady state phases is a major issue [?], because of the relationship between high performances and proximity to a stability limit. Core MHD modes are one of the key issues in the development and sustainment of transport barriers, as they degrade the confinement properties and, in the worse case, disrupt the plasma. The understanding of the underlying physics can provide the means of finding regimes without modes. In TCV (Tokamak à Configuration Variable) H-mode and eITBs have been obtained with different schemes, usually accompanied by various types of MHD phenomenon [?, ?, ?]. In this paper we focus on the ) low-shear Quasi-Stationary ELM free H-mode (QSEFHM) scenarios [?], which displays infrequent sawteeth and/or NTMs. In addition to that, high-performance eITBs shots are discussed, during which a variety of resistive to ideal modes ascribable to the infernal stability limit [?, ?]. Analysis of data from TCV highest performance discharges can clarify the potential threats of MHD modes in advanced scenarios. MHD core analysis of the QSEFHM [?], and of eITBs is presented, focusing on the existence of stability windows. The resulting operational stability limits are given, together with considerations regarding the projections of these results to a steady-state burning plasma.

## 1. Introduction

In TCV (Tokamak á Configuration Variable), thanks to the state-of-the-art ECH (Electron Cyclotron Heating) system, it is possible to locally modify the electron density and temperature profiles. Therefore, the current profile can be finely modified, with respect to the monotonic, Ohmic, one (due to neoclassical effects). Very small and reverse magnetic shear plasma are routinely obtained, examples of which are respectively the Quasi-Stationary ELM-Free H-Mode (QSEFHM, [?]) and high-performance eITBs (electron Internal Transport Barrier) discharges. Advanced scenarios, discussed in this paper, provide better confinement properties than conventional ones, mainly thanks to the reduced transport across flux surfaces, impeded by the arising of the transport barriers.

The main characteristic of H-mode QSEFHM discharges is the transition to an ELM-free phase, after the auxiliary heating is applied, much longer than the confinement time. This is not accompanied by the density and impurities peaking often observed in non-ELMy H-Modes, main drawback of the conventional ELM-free scenarios. In addition to that, the robustness of

the QSEFHM discussed in this paper makes it a potential candidate for future exploitation, subject to further understanding and investigation of its properties.

The formation and sustainment of eITB can also be accompanied by the development of MHD instabilities. The character of the observed instabilities varies from disruptive (infernal mode) to resistive (tearing mode developing magnetic island, classical or neoclassical). In addition, the MHD instabilities can cause periodic, spontaneous, slow, global oscillation of the plasma (electron temperature, density, plasma current, emitted radiation, etc). These are reminiscent of the Oscillatory Regime (O-regime [?]), which was first observed in the Tore Supra tokamak. In TCV the MHD and the O-regime are linked, with the first being the cause for the second[?].

MHD modes are detrimental for the confinement as they enhance perpendicular transport, and could be limiting the access to higher confinement, as in the case of discharges not developing the QSEFHM. Therefore, the study of the interplay between advanced scenarios and MHD activity is of crucial importance, as well as the way to avoid instabilities or to limit their effects.

## 2. The Quasi-Stationary ELM-Free H-Mode -*QSEFHM*-

In TCV H-mode are obtained with and without auxiliary electron cyclotron heating. The QSEFHM has been obtained in TCV by employing three gyrotrons at full power (1.41 MW, 118 GHz) with the vertical launcher on the third harmonic, X-polarization (X3). This regime appears to be of great relevance because it displays extremely good confinement properties, absence of ELMs, and absence of density and impurity peaking. In addition to that, the scenario is obtained with no momentum input, and in target plasmas that are fusion relevant ( $\beta \sim 2$ ,  $v_{eff} \sim 0.4$  and  $q_{95} = 2.5$ ), and expected in ITER. Finally, TCV is in the unique position across the tokamaks to be able to achieve H-mode heating the electrons, leaving the ions to be heated by ion-electron collisions, a scenario that mimics that of the burning plasma [?]. The QSEFHM (figure 1) is characterized by higher-than-normal  $D\alpha$  baseline emission compared to the Ohmic ELMy H-mode (top plot), high energy content (second plot), high constant plasma current (third plot, corresponding to  $q_{95} \sim 2.5$ ), approximately constant electron integrated density  $\bar{n}_e$  (fourth plot). The Ohmic ELMy phase begins at  $t \simeq 0.4$  s, characterized by small and frequent ELMs. These ELMs do not display any particular MHD precursor, although sawteeth activity is present, according to SXR measurement. The sawteeth crashes and the ELMs are not coupled. The X3 (third-harmonic, X-polarization Electron cyclotron heating launcher, [?]) heating starts at  $t = 0.6$  s, which causes the transition between the phases A and B in figure 1. At this time the increase in plasma energy is evident, from the energy trace (second plot, black trace) and the SXR emission (bottom plot). In this initial phase, the three gyrotrons are used at full power (third plot, red trace). At  $t = 0.8$  s, one of the three gyrotrons is power modulated ( $f = 240$  Hz), 30 ms before the QSEFHM begins ( $D\alpha$  emission, top plot). The ELMs become larger, and the frequency drops from 230 Hz to 60 Hz. The level of  $D\alpha$  emission (per ELM) doubles. The B-phase shows type-I ELMs, typically observed in TCV during the ECH H-mode transition. At  $t = 0.82$  s, the last ELM marks the beginning of phase-C, the quasi-stationary phase (QSEFHM). This phase does not show variation in the plasma current and averaged electron density. The plasma total energy (black trace, second plot) and electron energy (blue trace) reach their maximum value, which is kept stationary during the C-phase. At  $t \simeq 1.1$  s, a large ELM is seen from the  $D\alpha$  trace (top), which causes immediately a large drop in the SXR emission and a decrease in the energy. Conversely, the ELM does not cause any change in the averaged density. The ELM marks the transition between the first QSEFHM (C) and the second phase (D). Although at first sight these two appear to be identical (i.e. ELM free H-modes), the latter has a lower energy content.

The various levels of confinement properties can be better appreciated by following the evolution of the electron temperature and density profiles throughout the four phases of the QSEFHM discharge (figure 2). The top plot shows the spectrogram of the central soft X-ray signal (digitized at 200 kHz), showing a MHD mode whose onset is linked to the large ELM

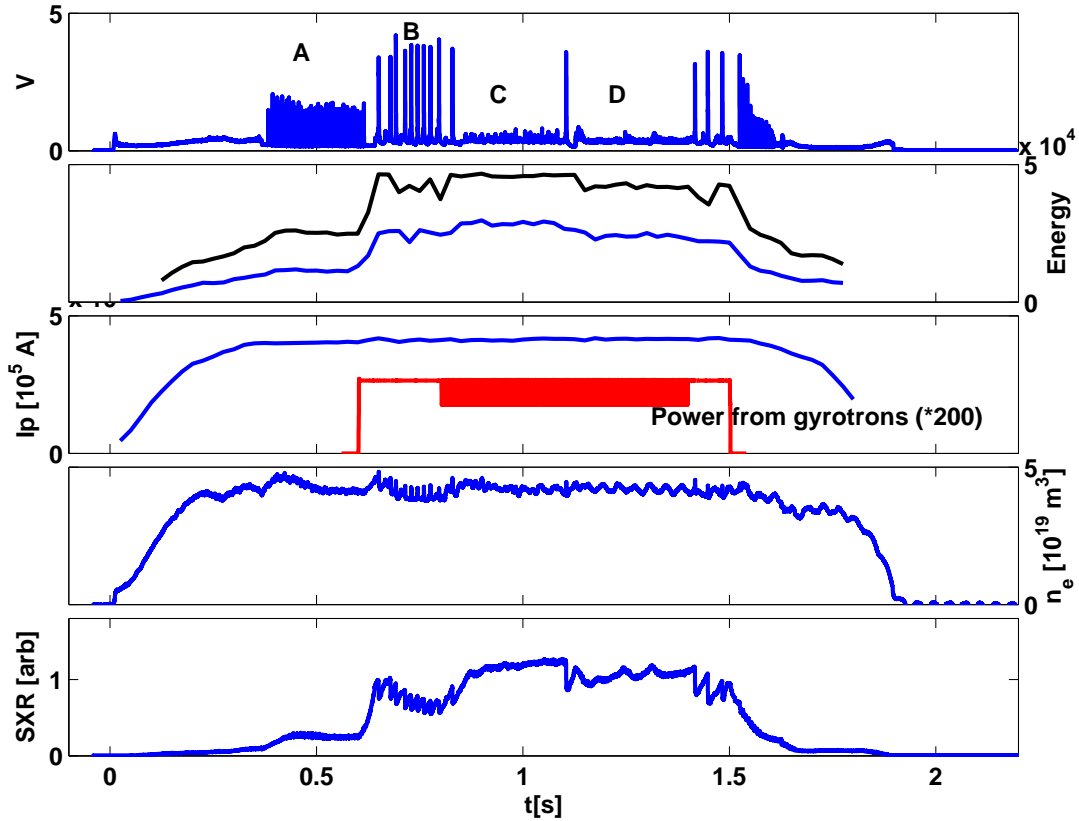


Figure 1. TCV Discharge #29892:

separating phase-C and D ( $D\alpha$  trace, blue). Four time windows are chosen during the four phases, characterized by different colors. The yellow profiles (electron density, bottom left; electron temperature, bottom right) represent the average Thomson Scattering profiles during the Ohmic ELMy H-mode. The density is as high as for the QSEFHM (no changes in the gas puffing are implemented during this phase), while the electron temperature is less than one third in the core. After the X3 heating is applied, the density slightly drops (-17%, larger ELMs) but the electron temperature strongly increases (magenta). The black vertical lines delimit the QSEFHM; during this phase the confinement properties are maximum for both the electron temperature and density, showing the high quality of this regime. The large ELM at  $t \simeq 1.1$  s triggers the NTM mode at  $f \sim 15$  kHz, which reduces the energy (also visible in figure 1, second plot) and the temperature is lower compared to the B-phase, whereas the density is higher, and their product is almost constant, suggesting that the effect of the NTM in the absence of ELMs is equivalent to the X3 heated, ELMy H-mode.

In the following subsection, a characterization of the MHD activity during the different phases is reported.

### 2.1. MHD characterization of the QSEFHM

The different phases (A to D) in terms of confinement behaves differently in terms of MHD activity, which plays an important role in defining the  $\beta$  value and therefore the level of energy in the plasma.

- **A:** During the Ohmic ELMy H-mode, typical small sawteeth are observed. These are sometimes seen in conjunction with precursors of the type  $m/n=1/1$  with frequency in the

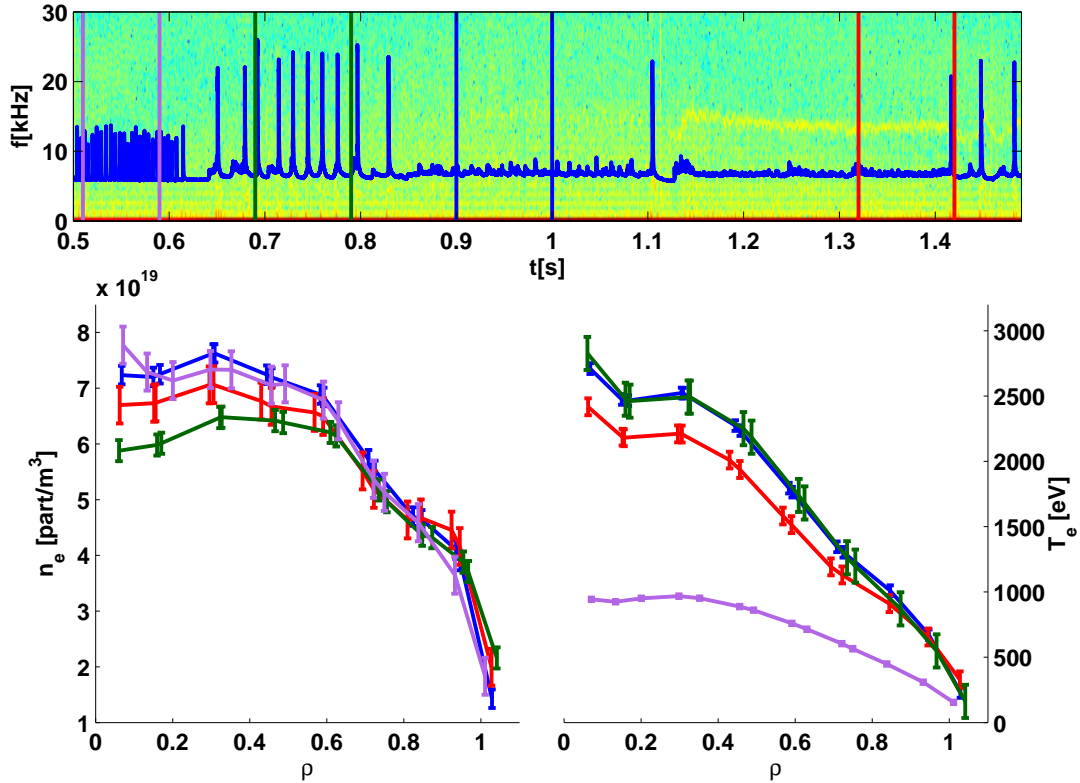


Figure 2. TCV Discharge #29892:

range 3-4 kHz; sometimes also short-lasting post-cursors are observed. The ELM activity is more rapid than the sawtooth one ( $f \sim 240$  Hz against  $f \sim 110$  Hz) and the two are de-correlated.

- **B:** In the X3 heated phase the ELMs are larger and with lower frequency. The core is stabilized against the sawtooth instability, although the soft X-ray raw traces at the ELM events is similar to that observed at sawtooth crashes. The radiation profiles in this case do not show any inversion radius, instead a global collapse is observed at every ELM. Preceding and following the ELMs, a coherent oscillation of the type  $m/n=2/1$  is observed from the magnetic probes and SXR diagnostic. This mode at  $f \sim 3$  kHz lasts for a few milliseconds after the crash, and it is then stabilized during the inter-ELM time, thus not having a significant impact on the confinement.
- **C:** During the C-phase, there is intermittent  $m/n=2/1$  activity (figure 3). The spectrogram of a magnetic toroidal Mirnov coil (top trace) shows the weak 5 kHz activity, which appears in bursts. The small crashes visible in the SXR trace (second plot), time zoom of the spectrogram (top plot, within vertical dashed lines), are likely to be related to the  $m/n=2/1$  mode, rather than being sawtooth crashes. This is because they appear together with the mode, and the inverted SXR profiles do not look like those typical of sawteeth. Furthermore, the size of the crash is almost negligible, in contrast with what is seen during the Ohmic phase (**A**) of the discharge. The  $D\alpha$  light remains at a higher baseline level (top plot, black trace), and little peaks are visible, generally appearing immediately after the SXR drops. This  $m/n=2/1$  mode mode is tiny, and cannot be finely resolved by the tomographic system. The higher resolution SXR diagnostic (DMPX), instead, can interpolate the inverted signal

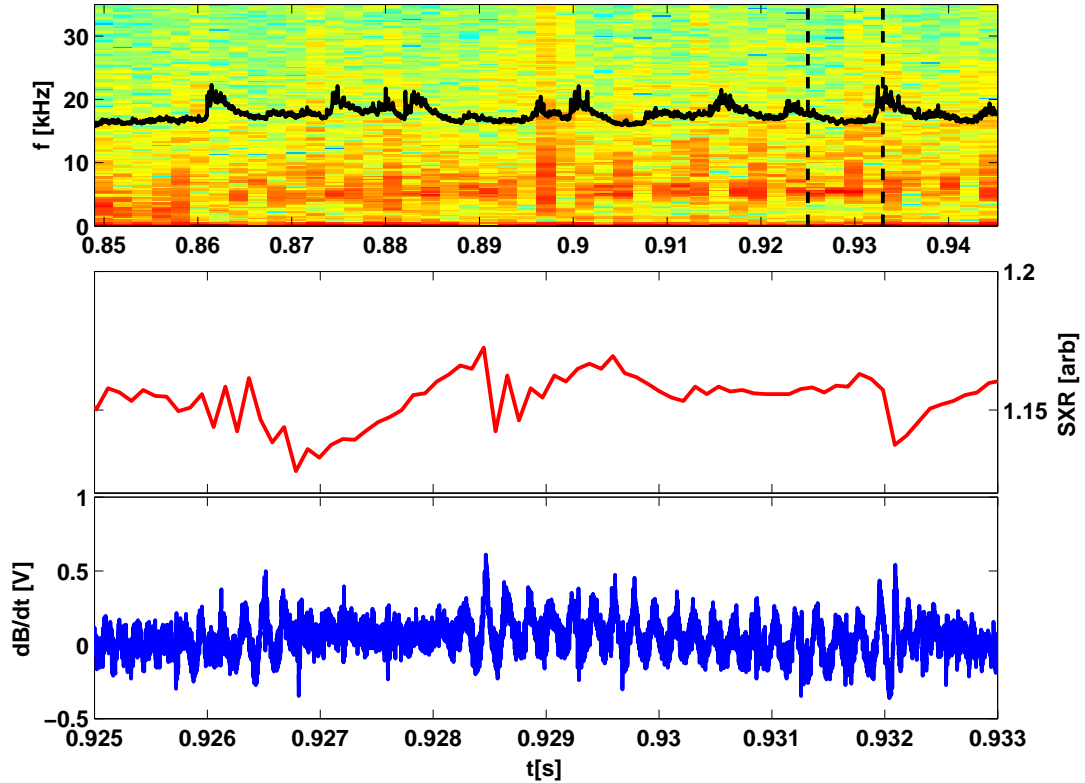
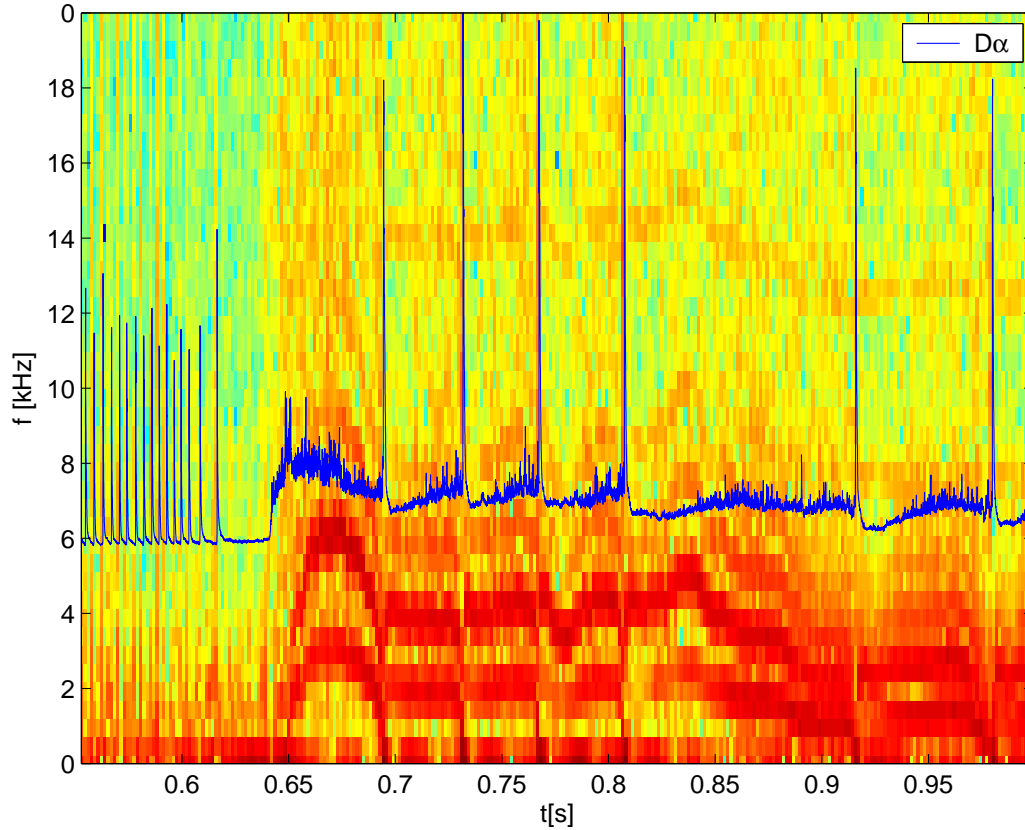


Figure 3. TCV Discharge #29892:

and agrees with the main magnetic poloidal periodicity being  $m=2$ . This is a further sign that the small crashes are not sawteeth.

- **D:** The D-phase is characterized by the single ELM event which triggers an NTM mode, with  $f \sim 15$  kHz. The MHD analysis reveal the periodicity of this mode to be mainly  $m/n=3/2$ . The island full width is approximately  $w \simeq 5$  cm. This corresponds to an expected drop in energy of  $\Delta W \sim 25\%$ , while the drop in electron energy from the reconstruction is  $\sim 20\%$  (figure 2). It has to be said that the absence of magnetic data at  $t \geq 1$  s, due to the fast (1 MHz) digitization chosen for this experiment, results in the use of solely DMPX for the discrimination of the island width. Although this reconstruction code has proved good reliability in the past when compared with magnetic data analysis, it tends in general to overestimate the island width by 15-20%. The resulting confinement level, from the electron energy calculations and the pressure profile from Thomson Scattering (TS) is comparable to that of the B-phase, i.e. that of an ELMy, X3-heated H-mode. The fact that the D-phase follows a major crash and survives the presence of an NTM mode is a sign that the QSEFHM is a fairly robust regime. This is a positive outcome for TCV and possibly for ITER, as this regime shows the advantages of an H-mode advanced scenario, without the disadvantages of the ELMs heat load on the divertor. On the other hand, the uncertainties regarding its attainment (in the following section a similar shot not developing the quasi-stationary regime is shown), and the potentially lethal singular ELM events require further studies to unveil the underlying physics of the stability properties of the QSEFHM.



**Figure 4. TCV Discharge #29894:**

### 2.2. Comparison between *ELMy X3 H-mode* and *QSEFHM*

Discharge #29894 (figure 4) was run with the same settings as discharge #29892 (QSEFHM), except that one of the gyrotrons in the latter was power modulated ( $f=230$  Hz) starting from  $t=0.8$  s. The pre-X3 phase for the two discharges are the same, with similar plasma current, electron density, plasma shape ( $l_i$ ,  $k$ ,  $\delta$ ). As soon as the X3 power is switched on, a large  $m/n=3/2$  mode appears at low frequency ( $f \simeq 6$  kHz). In discharge 29894 the mode rotation speeds up during the ELM-free phase lasting for approximately a confinement time ( $t \sim 50$  ms), and then it slows down just before the first ELM. At the ELM event the frequency spectrum shows a step deceleration of the mode, which is repeated for all the other ELMs, all of which separated in time by approximately a confinement time. The  $m/n=3/2$  mode is non-linearly coupled with the  $m/n=2/1$  at  $f \simeq 3$  kHz. The mode closer to the core, i.e. the one at the  $q=1.5$  resonant surface, is the dominant one. From a bi-coherence analysis (figure 5) it is possible to verify if the coupling (if any) of the two modes. The analysis consider the frequency relation between two coherent modes and the phase information within the Fourier transformation in the frequency space ???. In figure 5 the correlation level between the frequencies of the two modes is approximately 0.7 at the frequency equal to the combinations of the two modes fundamental frequencies,  $f_1 \pm f_2$ . This means that the two modes are locked, i.e. they are rotating in such a way that the phase is not mixed (the phase difference between the two remains constant). The confirmation of the existence of two separate, locked modes, is also obtained through magnetic island modeling ??, where current filaments are simulated on the flux surfaces reconstructed

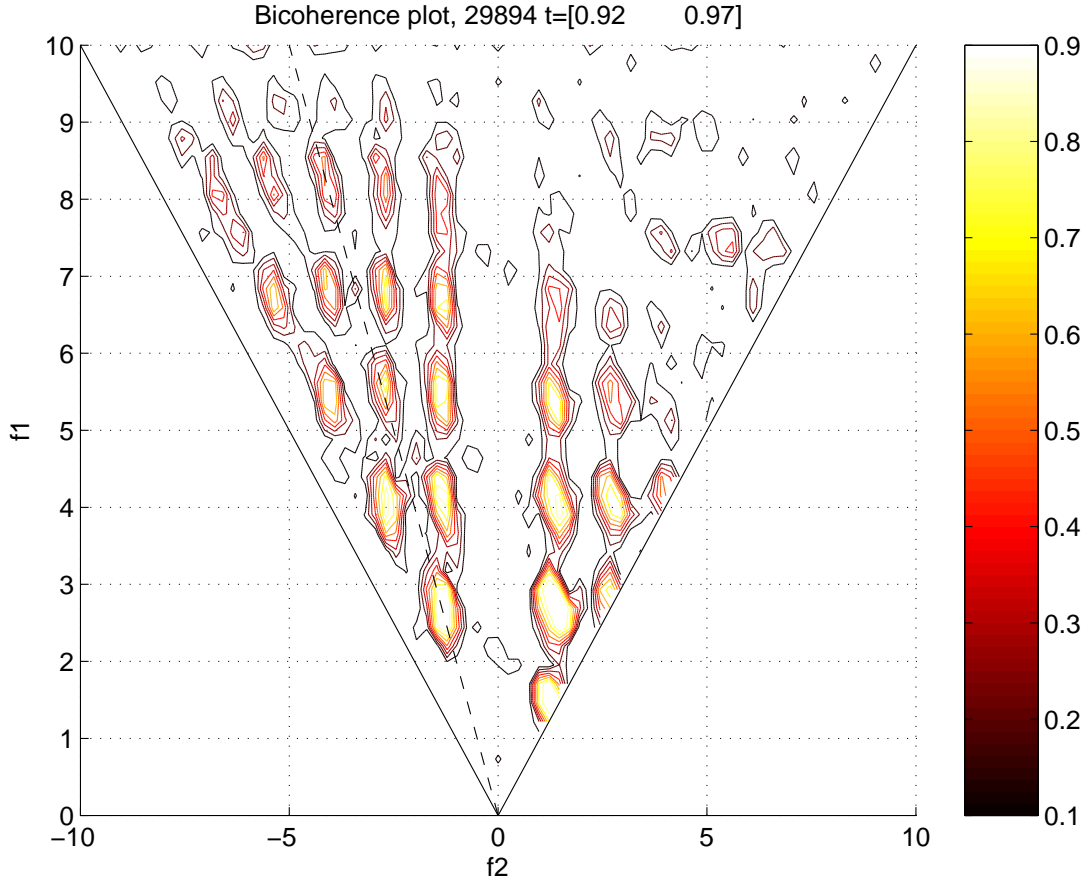


**Figure 5. TCV Discharge #29894:**

with the LIUQE ?? code. The perturbed magnetic field is then extrapolated to the poloidal magnetic coils placed around the vessel at different poloidal locations. The result gives the degree of confidence on the mode poloidal periodicity, which is mainly  $m=3$ . Furthermore, at a later time the lower frequency mode ( $m/n=2/1$ ) is stabilized after an ELM for 50 ms, whereas the dominant  $3/2$  is not. The bi-coherence plot during this time interval does not show any similarities with that obtained during the times when the two modes are coexisting (figure 5), further indicating the presence of locked  $3/2$  and  $2/1$ , with the first being the dominant one. Figure 6 shows the DMPX reconstruction of the modes, showing the iso-surface of perturbed SXR emission for the  $m/n=3/2$  mode. The black lines represent the maximum extent of the  $m/n=2/1$  mode, for which the interpolation returns a larger error. Hence, these are the extremes  $\rho_s$  occupied by the external island. This reconstruction is useful to add resonance points on the q-reconstruction by LIUQE (figure 8). The diamond represent the best fit for the DMPX signals, and the horizontal line is an error-bar  $\pm 7\%$  of the central location, with this value chosen according to profile inversion simulation. This is useful to provide further constraints when running plasma transport simulations.

The effect of the mode can be observed through the detailed comparison of the averaged Thomson Scattering profiles during different phases of the discharges (figure 7).

- **(Black)**: during the Ohmic ELMy phase, before the development of the  $m/n=3/2$  mode, the two pressure profiles (bottom-left plot) are overlapped, meaning that the discharge in that phase is developing in the very same manner. Indeed, the only difference in the

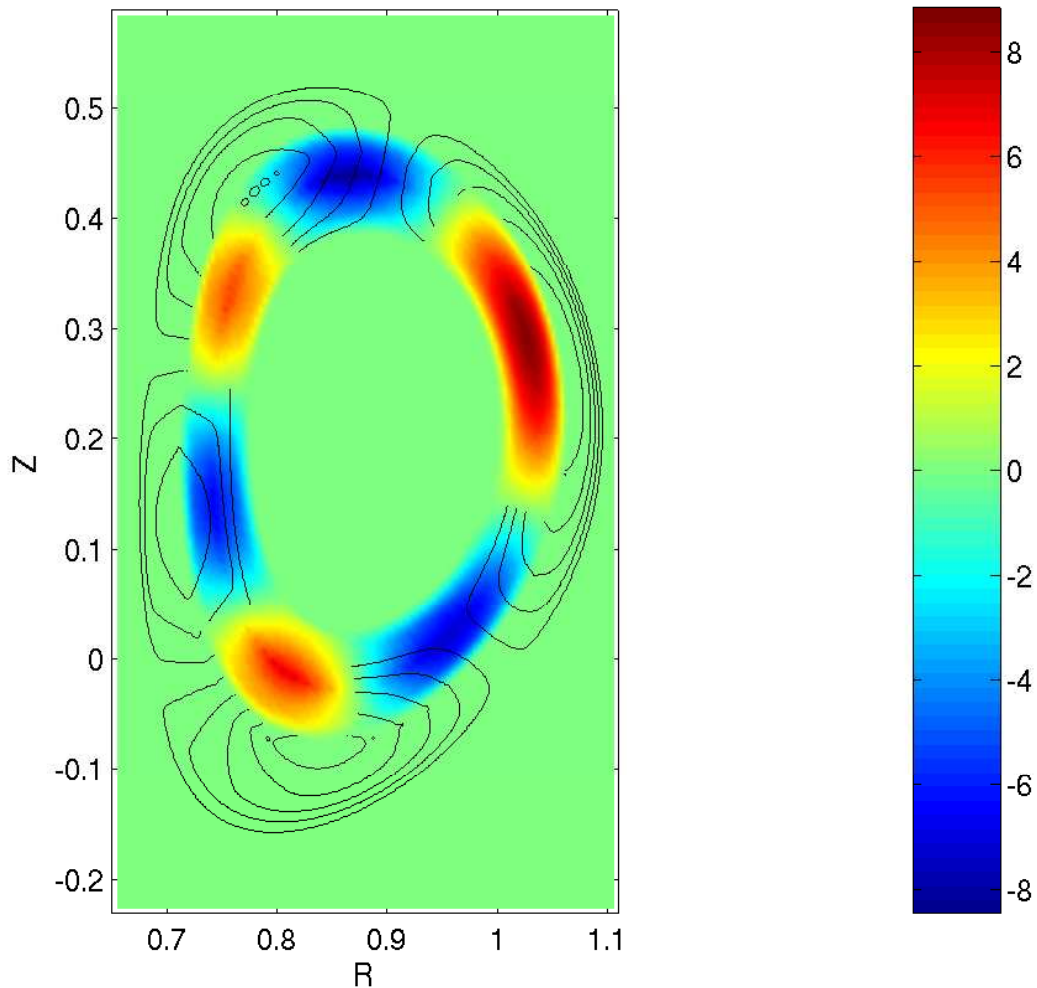


**Figure 6. TCV Discharge #29894:**

setting-up of the discharges is the modulation of the power, which is turned on at  $t=0.8$  s.

- **(red)**: as soon as the X3 heating is commenced, discharge 29894 (second spectrogram from the top) shows the coupled modes, together with ELMs; Discharge 29892, instead, only the ELMs and sawtooth activity. The result, in terms of confined electron pressure, is an increase of the pressure for both discharges (due to the X3 heating), with discharge 29892 more than doubling the Ohmic-phase pressure, while 29894 (dashed line with diamonds) reaching a maximum that is 25% less than for 29892. This is the effect of the island (width  $\approx 7$  cm), which is estimated in a loss of 33% of confinement, in agreement with the pressure drop. As the QSEFHM appears to be related to the available power and the quality of confinement, it is possible that it is this lack of  $\beta$  properties for 29894 (and similar shots) to reduce the probabilities to enter the quasi-stationary state. This statement requires further investigation, and further experiments are planned for the next TCV campaign.
- **(cyan ,yellow)**: the variation in the confined pressure for discharge 29894 are negligible between the three phases. The mode is visible throughout the whole discharge, during X3 heating, with the frequency slowing down at  $t=0.9$  s, and after that rotating stably at



approximately  $f=3$  kHz ( $m/n=3/2$  mode). An interesting comparison is between the two discharges during the yellow phase. Both plasmas have a NTM-like mode, but the size and frequencies are rather different, and so are the effects on confinement. In 29892 the NTM is retained in the plasma for approximately 8 confinement times without causing a major collapse of the profiles. The plasma pressure is still 25% higher than that for the non-QSEFHM discharge, i.e. the same difference observed during the X3 ELMy phase (red) without NTM (29892) in comparison with the ELMs plus the onset of the mode for 29894.

### 2.3. Summary on the H-mode and QSEFHM

Ohmic and ECH heated H-modes are routinely obtained on TCV, displaying type-I ELMs and other types of MHD instabilities. If X3 power is injected from the top, and the conditions in terms of plasma parameters and shape are met (together with the absence of large MHD modes) the plasma can access a quasi-steady ELM-free H-mode (QSEFHM), with better confinement properties and absence of ELMs. The reasons for the attainment (or not) of this regime are still unknown, and further experiments are planned. The positive aspects are the absence of ELMs, the improved confinement, the robustness of the regime and the absence of density peaking. On the other hand, the regime cannot be easily reproduced and sometimes large ELMs are seen to interrupt the quasi-stationary phase, inducing a threat for the maximum thermal load and the possibility of triggering NTMs. MHD stability plays a fundamental role, since discharges without large magnetic islands have confinement properties up to 40% higher than similar discharges with modes. In addition, no discharge has been found (up to this time) that develops the QSEFHM

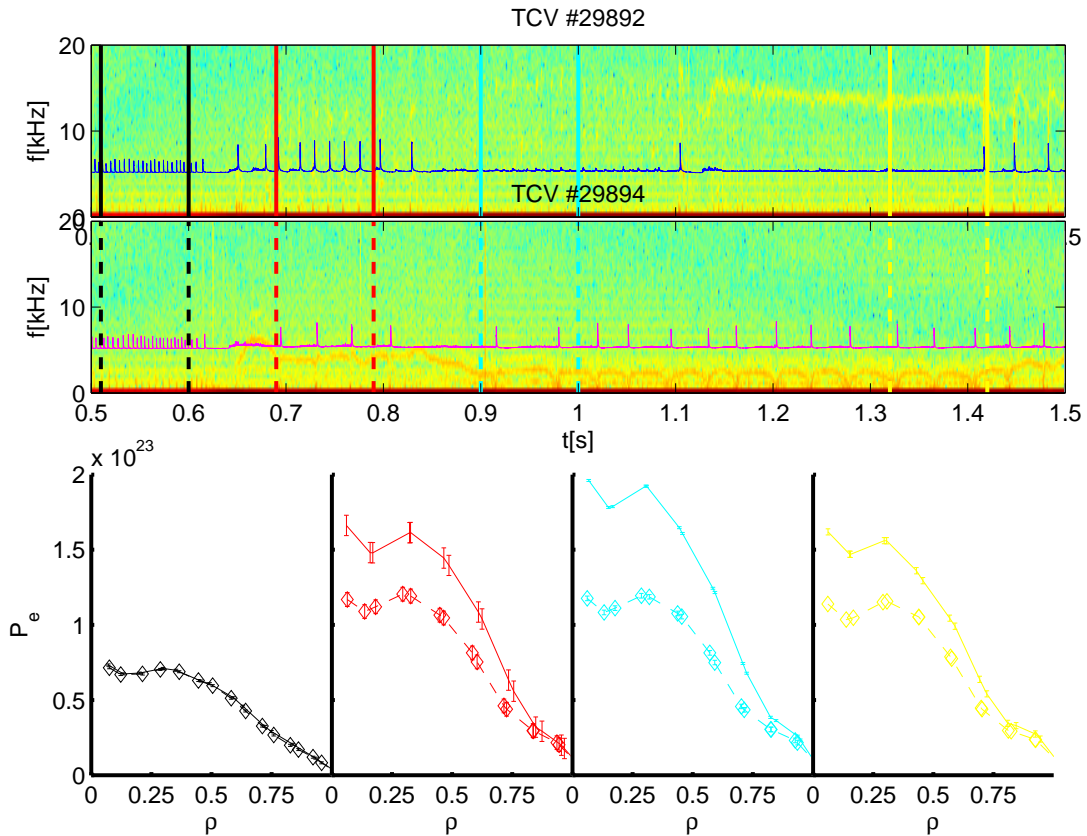
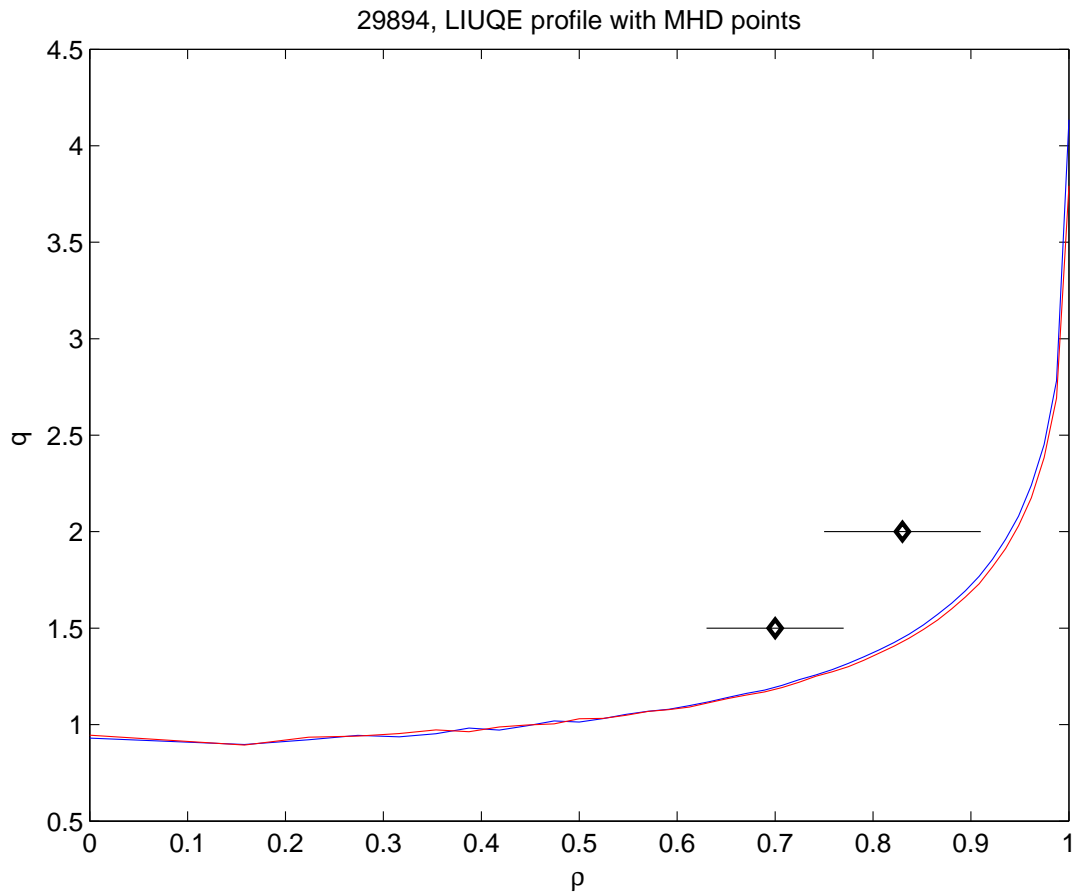


Figure 7. TCV Discharge #29894:



**Figure 8. TCV Discharge #29894:**

when the X3 heating triggers a mode on the  $q=1.5-2$  rational surfaces. Understanding the interplay of core MHD with the scenario achievement (if any), and the stability properties of X3 heated ELMs is a key factor for the reproducibility and safe operation of the QSEFHM.

### **3. Bibliography**